ACS OMEGA

Open Access

http://pubs.acs.org/journal/acsodf

Article

Spectral Analysis on Cuba-Lumacaftor: Cubane as Benzene Bioisosteres of Lumacaftor

Dongdong Wang,[‖] Xiaohong Lyu,[‖] Mengtao Sun,* and Yongqiang Liang*

Cite This: *ACS Omega* 2023, 8, 43332−43340

Read Online

ACCESS | Metrics & More | Article Recommendations

ABSTRACT: In this paper, we theoretically investigate the electronic structure and physical properties of cuba-lumacaftor, cubane as benzene bioisosteres of lumacaftor, stimulated by recent experimental reports [Wiesenfeldt, M. P.; et al. *Nature* **2023**, *618*, 513−518]. The permanent electric dipole moments of cuba-lumacaftor in neutral, acidic, and alkaline environments are significantly enlarged than that of lumacaftor, significantly promoting the interaction between cuba-lumacaftor and surrounding polar solvent environments and resulting in pH-independent high solubility and pharmacological activity. Furthermore, electronic circular dichroism (ECD) spectra reveal that the chirality of cuba-lumacaftor is much decreased compared to that of lumacaftor. Raman spectra and resonance Raman spectra combined with polarizability also reveal the vibrational information on cuba-lumacaftor. Our results promote a deeper understanding of better pharmacological activity.

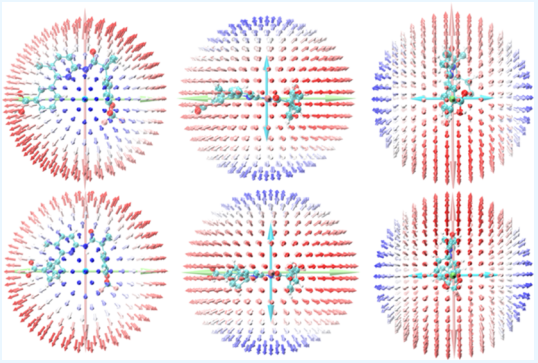

1. INTRODUCTION

Lumacaftor[1] (see Figure 1a) is in a group of medications entitled cystic fibrosis transmembrane conductance regulator (CFTR)[2] correctors. As a protein chaperone, lumacaftor is used in amalgamation with ivacaftor[3] to treat homozygous patients' cystic fibrosis (CF),[4] which is an inborn disease of the mutation in the CFTR gene and results in difficulties with digestion, breathing, and reproduction. Ivacaftor is in a variety of medications termed CFTR potentiators. Both lumacaftor and ivacaftor can improve the protein function in order to decrease the accumulation of thick mucus in the lungs and refine other CF symptoms.[1] It is one of the urgent issues to promote the pharmacological activity of lumacaftor, in which bioisosteric replacement is one of the candidate solutions.[5]

The replacement of benzene rings with sp^3-hybridized bioisosteres in drug candidates normally improves pharmacokinetic properties, such as metabolic stability and solubility, by reducing the overall C(sp^2) character while retaining biological activity.[5−7] Cubane is an ideal bioisostere because it affords the closest geometric suit to benzene.[8,9] The rigid ring strain of cubane imparts high strength of bond and then metabolic stability on cubane's C−H bonds.[10−12] To improve the solubility of lumacaftor and increase the metabolic stability of lumacaftor, bioisosteric replacement of the benzene ring of lumacaftor with a cubane is proposed,[5] cuba-lumacaftor (see Figure 1b). The bioisosteric replacement of the benzene ring with a cubane is of pH-independent high solubility, which can improve absorption of the compound through the gastrointestinal tract; furthermore, cuba-lumacaftor can increase metabolic stability.[5] Until now, the physical mechanism behind the highly pharmacological activity in different pH environments has not been clearly elucidated, which necessitates an urgent theoretical investigation. Also, the Raman spectroscopy of cuba-lumacaftor is also very valuable in investigating its physical properties, since Raman spectroscopy is very sensitive to the change of molecular structures and provides vibrational information on bioisosteric replacement in different pH environments.

In this work, we theoretically investigate the electronic structures and physical and chemical properties of lumacaftor and cuba-lumacaftor to indicate the advantages of cuba-lumacaftor over lumacaftor, based on the recent experimental reports in ref 5. The chirality of lumacaftor and cuba-lumacaftor are also discussed in detail by means of electronic circular dichroism (ECD) spectra. Our results provide a deeper understanding of the bioisosteric replacement of the benzene ring of lumacaftor with a cubane.

Received: September 29, 2023
Revised: October 13, 2023
Accepted: October 20, 2023
Published: November 3, 2023

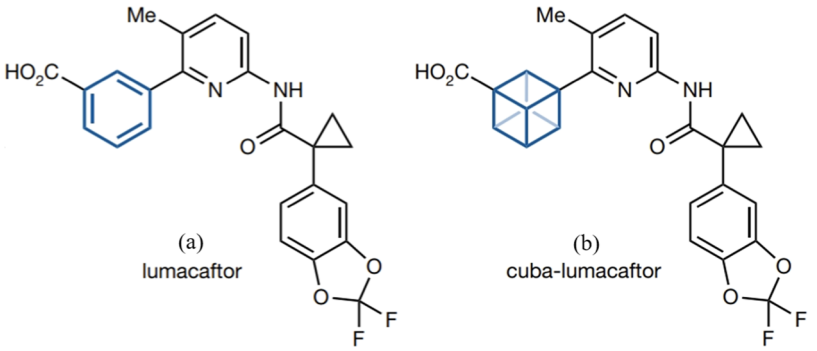

Figure 1. Molecular structures of (a) lumacaftor and (b) cuba-lumacaftor.

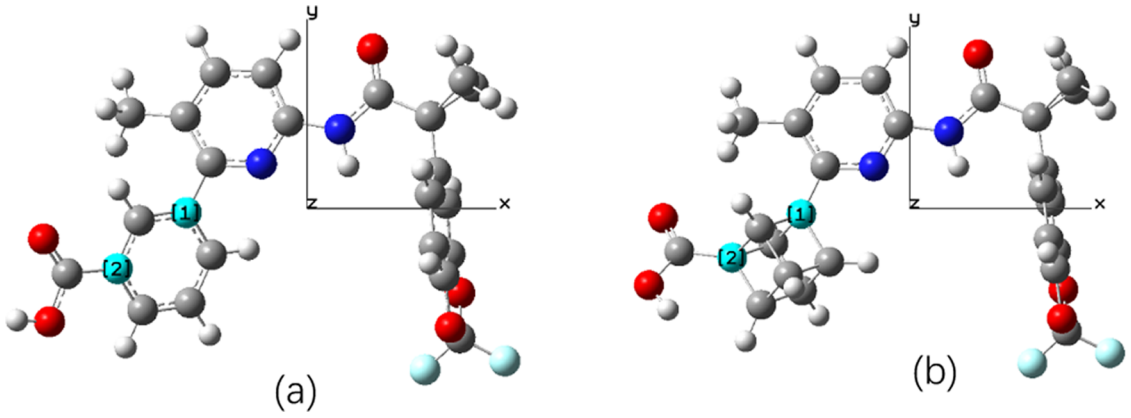

Figure 2. Geometric structures of (a) lumacaftor and (b) cuba-lumacaftor.

2. METHODS

All theoretical calculations were done by Gaussian 16 software.[13] Molecular geometries (see Figure 1) were optimized with density functional theory (DFT),[14] Becke-3−Lee−Yang−Parr (B3LYP) functional,[15] and 6-31G(d) basis set.[16] Their Raman spectra and nuclear magnetic resonance (NMR) are also calculated at the same level of theory. The absorption spectra, resonance Raman spectra, and ECD were calculated with time-dependent DFT (TD-DFT),[17] CAM-B3LYP functional,[18] and 6-31G(d) basis set, which is suitable to calculate ECD spectra.[19,20]

3. RESULTS AND DISCUSSION

The optimized geometries of lumacaftor and cuba-lumacaftor can be seen in Figure 2. The distance of lumacaftor and cuba-lumacaftor between atoms 1 and 2 are 2.44 and 2.25 Å (see Figure 2), respectively, which confirms that cubane affords the closest geometric suit to benzene. Furthermore, the other fragment geometries are kept unchanged. The electrons on the benzene rings of lumacaftor and on the cubane of cub-lumacaftor are −0.131e and −0.055e, respectively. The detailed difference of electrons on the atoms of lumacaftor and cuba-lumacaftor results in the large difference of permanent electric dipole moments (μ) between two molecules on the ground state. The replacement of the benzene ring by cubane results in a significant increase of permanent dipole moments of cuba-lumacaftor compared with that of lumacaftor; see blue vector arrows in Figure 3a,b, and detailed data are listed in Table 1. Molecular permanent electric dipole moments play a crucial role in determining the polar permutation between drugs and solvents and improving the high solubility. The larger permanent dipole moments can result in stronger interaction with environmental polar solvents, which is one of the reasons that cuba-lumacaftor improves absorption of the compound through the gastrointestinal tract and increases metabolic stability. To reveal that cuba-lumacaftor is of pH-independent high solubility, the protonation and deprotonation of cuba-lumacaftor in acidic and alkaline environments and the permanent electric dipole moments of protonated and deprotonated cuba-lumacaftor are also calculated, see Figure 3c,d and data in Table 1. Though the orientation of permanent electric dipole moments is changed, the numeric value is almost unchanged for the protonation of cuba-lumacaftor in acidic environments. The deprotonation of cuba-lumacaftor in alkaline environments significantly enhances the permanent electric dipole moment. Thus, in alkaline environments, cuba-lumacaftor can interact more effectively with an environmental polar solvent.

The replacement of benzene rings by cubane, the orbital energy level, and density of state (DOS) Frontier molecular orbits (FMOs) of lumacaftor and cuba-lumacaftor are significantly different; see Figure 4a; in general, the orbital energy levels of cuba-lumacaftor are higher than that of lumacaftor. Furthermore, the DOSs for highest occupied molecular orbital (HOMO) and least unoccupied molecular orbital (LUMO) display different distributions across molecular fragments; see Figure 4b,c. Both energy levels and DOS of cuba-lumacaftor indicate that the pharmacological activity of cuba-lumacaftor may be stronger than that of lumacaftor. This is due to the presence of higher orbital energies in the HOMO and LUMO levels of cuba-lumacaftor, which indicates potentially higher reactivity.

https://doi.org/10.1021/acsomega.3c07532
ACS Omega 2023, 8, 43332−43340

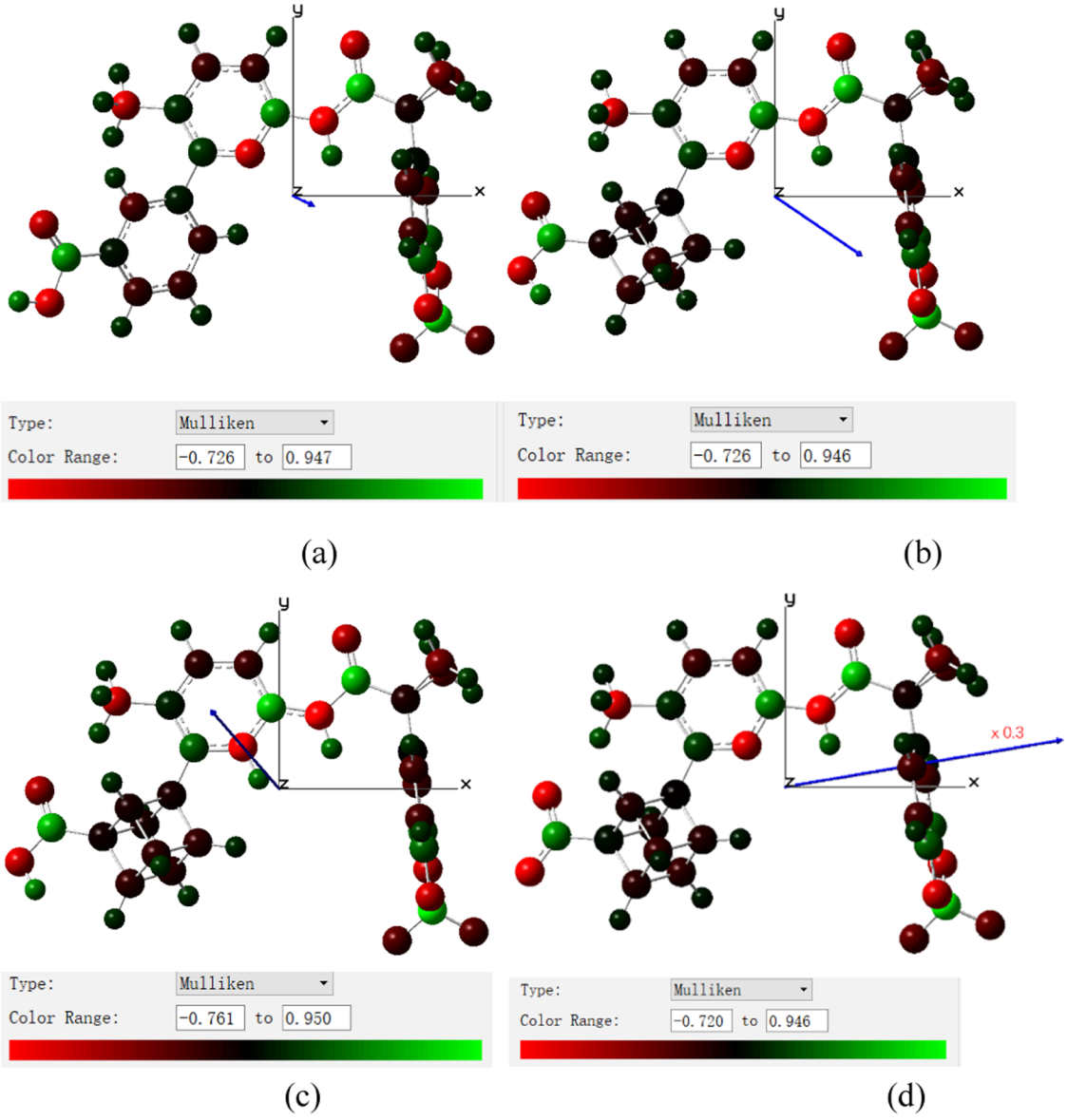

Figure 3. Charge distribution and permanent electric dipole moments of (a) lumacaftor and (b) neutral, (c) protonated, and (d) deprotonated cuba-lumacaftor.

Table 1. Permanent Electric Dipole Moments of Lumacaftor and Cuba-Lumacaftor, and the Unit is Debye

		x	*y*	*z*
lumacaftor	neutral	0.63	−0.30	0.33
cuba-lumacaftor	neutral	2.49	−1.70	3.10
	protonated	−1.93	2.22	3.20
	deprotonated	25.75	4.37	3.62

Figure 5 demonstrates the energy levels of cuba-lumacaftor in different pH environments. By comparing the distribution of DOSs on the HOMO and LUMO of neutral and protonated cuba-lumacaftor, it is found that the DOSs of HOMO and LUMO exchange each other; thus, the orientation of permanent electric dipole moments are opposite in *x* and *y* in Figure 3b,c, and see data in Table 1. Also, when cuba-lumacaftor is deprotonated in an alkaline environment, the orbital energy levels of both HOMO and LUMO highly increase, and the DOSs on HOMO and LUMO are significantly localized on different fragments, which results in the larger permanent electric dipole moments and can significantly increase the interaction between cuba-lumacaftor with solvents in surrounding alkaline environments and increase solubility, as well as pharmacological activity.

The chirality of drugs can strongly influence pharmacological activity, as different enantiomers may exhibit different functions in various metabolic pathways. ECD is a spectroscopic technique that obtains information by measuring the difference in the absorption of molecules under left-handed circularly polarized light and right-handed circularly polarized light. In the ECD measurement, both left-handed circularly polarized light and right-handed circularly polarized light are simultaneously irradiated onto chiral molecules. When these two types of light pass through, the light they interact with molecules will be different. This is because the configuration of chiral molecules requires different energies to absorb left-handed circularly polarized light and right-handed circularly polarized light in different directions. By measuring the difference in absorption of left-handed circularly polarized light and right-handed circularly

https://doi.org/10.1021/acsomega.3c07532
ACS Omega 2023, 8, 43332−43340

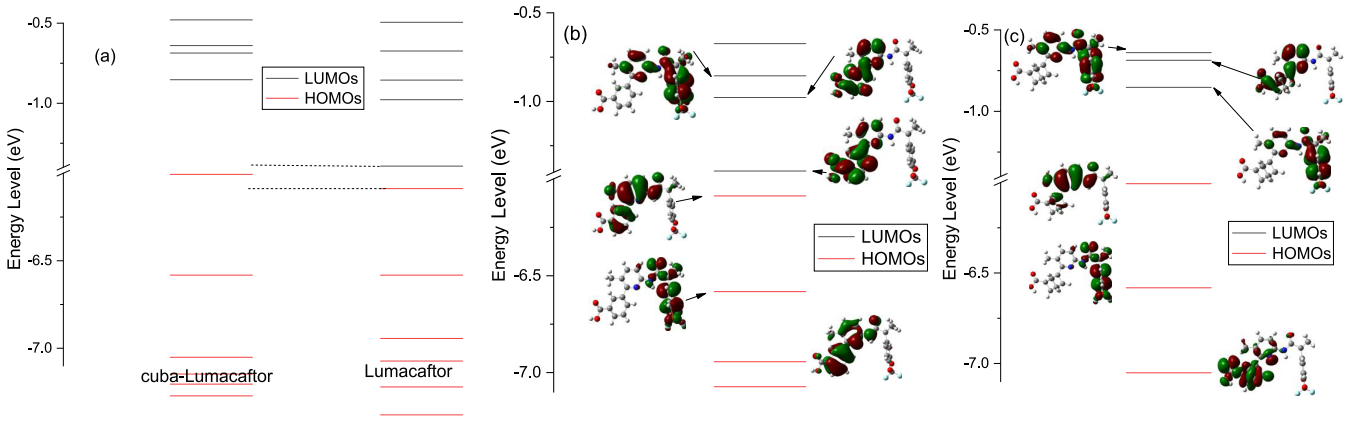

Figure 4. (a) Comparison between the frontier molecular orbits (FMOs) of lumacaftor and cuba-lumacaftor. (b) FMOs and DOS of lumacaftor. (c) FMOs and DOS of neutral cuba-lumacaftor.

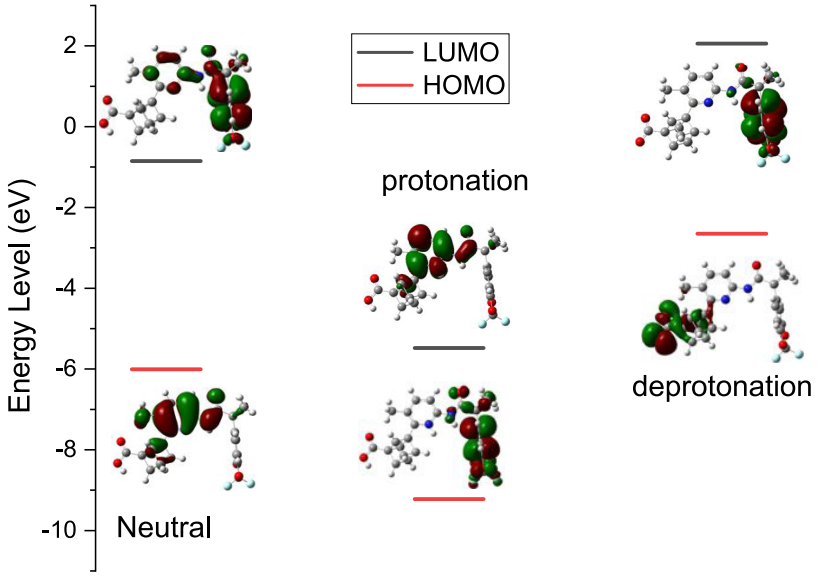

Figure 5. Energy levels of cuba-lumacaftor in different pH environments.

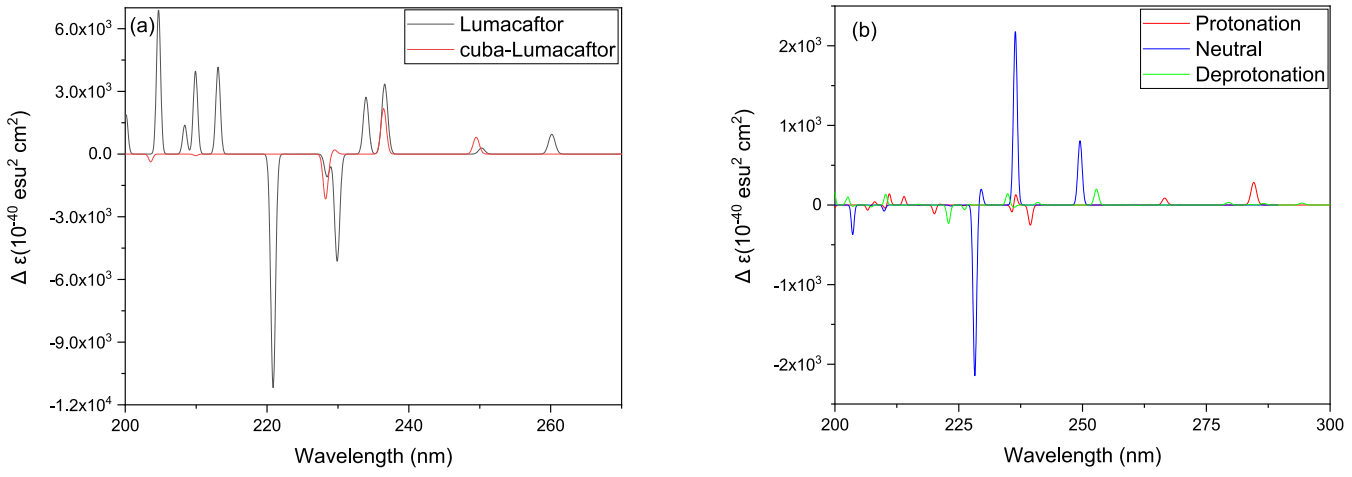

Figure 6. (a) ECD spectra of neutral lumacaftor and cuba-lumacaftor and (b) ECD spectra of cuba-lumacaftor in different pH environments.

polarized light by chiral molecules, the ECD spectra can be obtained. A positive ECD spectrum indicates that the absorption intensity of left-handed circularly polarized light is greater than that of right-handed circularly polarized light, while a negative ECD spectrum indicates that the absorption intensity of right-handed circularly polarized light is greater than that of left-handed circularly polarized light. Figure 6a demonstrates the chirality of lumacaftor and cuba-lumacaftor demonstrated by

https://doi.org/10.1021/acsomega.3c07532
ACS Omega 2023, 8, 43332−43340

ECD spectra, and it is found that the chirality of cuba-lumacaftor is significantly decreased compared with that of Lumacaftor. The decrease in chirality may change the pharmacological activity.[21,22] Figure 6b shows that in acidic and alkaline environments, the chirality of the protonated and deprotonated cuba-lumacaftor further significantly decreases.

Raman spectroscopy is an ultrasensitive spectral analysis method to reflect molecular vibrational information. Figure 7 demonstrates the Raman spectra of lumacaftor (Figure 7a) and cuba-lumacaftor (Figure 7b), and the vibrational modes of the benzene ring of lumacaftor and cubane of cuba-lumacaftor are shown. The Raman peaks of the benzene ring of lumacaftor in Figure 7a disappear in Figure 7b, and the Raman peaks of cubane of cuba-lumacaftor appear in Figure 7b.

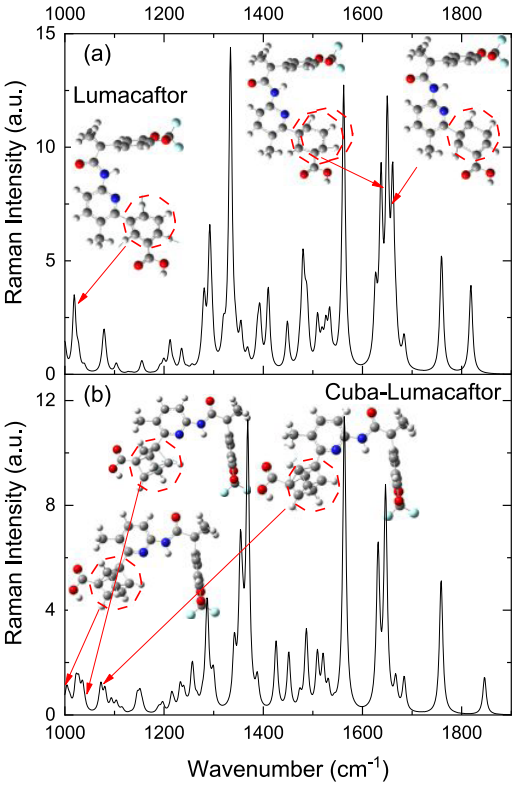

Figure 7. Raman spectra of (a) lumacaftor and (b) cuba-lumacaftor; the inset shows the vibrational modes of Raman spectra.

Since Raman intensity follows the relation $I = \alpha^2 E^4$, the visualization of polarizability in three different orientations can reveal the difference in the cubane unit, as shown in Figure 8. The blue, white, and red colors represent the polarizability from small to large. The arrows on the spherical surface in the figure represent the change in the dipole moment of the molecule when the center of the molecule applies an external electric field of the same strength in all directions. The green, pink, and light blue long arrows are the general trend of the polarizability of the system along three different orientations. It is found that the polarizability around the cubane unit is slightly stronger than that around the benzene unit. In general, there is not too much difference between two molecular polarizabilities, which reflects that the profile of their Raman spectra is little different, especially on weak Raman intensities of the vibrational modes of cubane and benzene parts from 1000 to 1100 cm^{-1}.

It is necessary to reveal the Raman spectra of cuba-lumacaftor in different pH environments. Raman spectra of neutral, deprotonated, and protonated cuba-lumacaftor are calculated; see Figure 9, which demonstrates that their profiles are slightly different. Also, the vibrational modes of cubane are of weak Raman peaks from 1000 to 1100 cm^{-1}.

To study the polar effect of solvent, the electronic structure of cuba-lumacaftor in the polar water solvent is calculated; see Figure 10a. It is found that the difference in the energy levels of HOMO and LUMO increases, and the DOS of LUMO in the water solvent is delocalized, which results in the larger permanent electric dipole moment; see data in Table 2. Furthermore, the permanent dipole polarizability also increases in water; see data in Table 2. Since the Raman intensity is determined by permanent dipole polarizability, the Raman intensity of cuba-lumacaftor in polar water solvent can be significantly enhanced and red-shifted at high frequencies; see Figure 10b. Also, the ECD spectra indicate that in the polar water solvent, the chirality intensity significantly decreases; see Figure 10c. The chirality can significantly influence the pharmacological activity.[21,22]

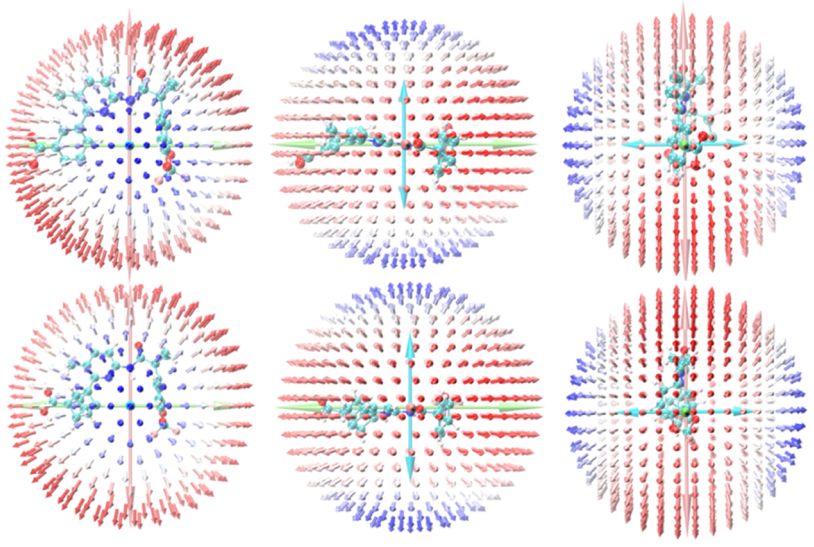

Figure 8. Visualizations of the static polarizabilities of lumacaftor and cuba-lumacaftor in different orientations.

https://doi.org/10.1021/acsomega.3c07532
ACS Omega 2023, 8, 43332−43340

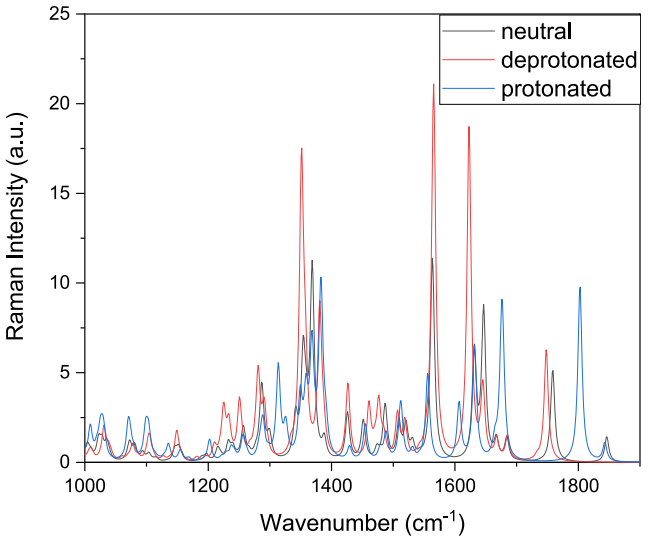

Figure 9. Raman spectra of neutral, deprotonated, and protonated cuba-lumacaftor.

In Figure 7, the intensity of the normal Raman peak is weak, especially on the vibrational modes of the cubane unit in the region from 1000 to 1100 cm^{-1}. To clearly observe the Raman intensities and the vibrational modes of the cubane unit, the resonance Raman spectra of cuba-lumacaftor are calculated (see Figure 11) by excitation on the S_1 and S_3 excited states in the absorption spectrum in Figure 11. The inset in Figure 11 shows that cubane is a donor of electrons in electronic transitions, where green and red stand for holes and electrons, respectively.

Figure 12a,b demonstrates that molecular resonant Raman spectra can be significantly enhanced by the resonance excitations compared with static Raman spectra in Figure 7; this enhancement is known as chemical enhancement.[22] The strongest resonance Raman peaks around 1400 cm^{-1} are cubane vibrational modes; see the inset in Figure 12b. The profiles of resonance Raman spectra in Figure 12 are significantly different from the normal Raman spectrum in Figure 8 due to the charge transfer resonance excitation.,[22 23] By comparing Figure 12a,b, we can find that the resonance Raman spectrum excited by 250 nm is better for observing the vibrational mode of the cubane unit, which is the strongest intensity of the Raman peak in Figure 12b.

To further reveal the significant differences in resonance Raman spectra excited by different excitation wavelengths, the dynamic polarizability excited by different lights is shown in

Table 2. Permanent Electric Dipole Moments of Lumacaftor and Cuba-Lumacaftor, and the Unit is Debye

	x	*y*	*z*	*xx*	*yy*	*zz*
no solvent	2.49	−1.70	3.10	325.1	328.3	201.0
in water	2.71	−2.37	4.77	401.9	433.0	284.3

Figure 13, where the blue, white, and red colors represent the polarizability from small to large. The arrows on the spherical surface in the figure represent the change in the dipole moment of the molecule when the center of the molecule applies an external electric field of the same strength in all directions. The green, pink, and light blue arrows are the general trend of the polarizability of the system along three different orientations. It is found that they are significantly different, which results in the significantly different profiles of resonance Raman spectra in Figure 11.

NMR spectra are a commonly used technique for analyzing the structures and properties of substances. It is based on the resonance phenomenon of atomic nuclei under an external magnetic field. The horizontal axis represents the chemical shifts. The right vertical axis represents the relative signal strength of the spectral peak, which is usually dimensionless. It is used to represent the intensity of each nuclear resonance peak. The left vertical axis represents degeneracy, indicating the overlap or multiplicity of the spectral peaks. When two or more different nuclei have very similar chemical shifts (or resonance frequencies) in the nuclear magnetic resonance spectrum, their peaks appear at similar positions and overlap together. This overlapping phenomenon is referred to as degeneracy. The height of the black vertical line in Figure 14 corresponds to the coordinate axis on the left, which represents degeneracy. As the chemical shifts of all of the carbon atoms currently differ significantly, the degeneracy is 1. The red line in the figure is obtained by widening the black vertical line using the Lorentz function, and its value corresponds to the coordinate axis on the right. Figure 14 demonstrates the NMR spectra of the cubane unit of cuba-lumacaftor, and the labels of the cubane unit circled by a red ring are shown in the inset in Figure 14, where the H atoms are not shown. The chemical shifts of the C atoms of the cubane unit are mainly in the region from 35 to 55 ppm. C atom #1 of the cubane unit shows the largest chemical shift.

4. CONCLUSIONS

The electronic structure and physical properties of cuba-lumacaftor were theoretically investigated. The significantly

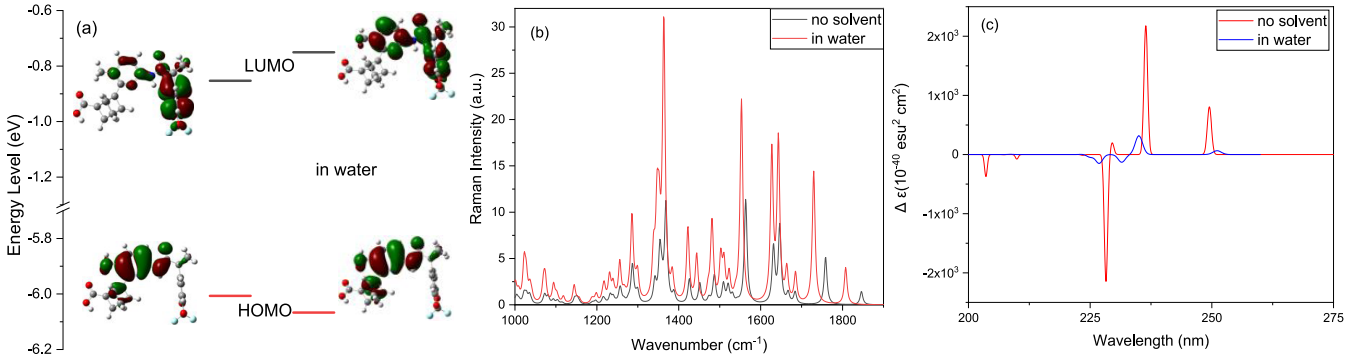

Figure 10. Electronic structure and Raman and ECD spectra of cuba-lumacaftor in the polar water solvent: (a) energy levels, (b) Raman spectra, and (c) ECD spectra.

https://doi.org/10.1021/acsomega.3c07532
ACS Omega 2023, 8, 43332−43340

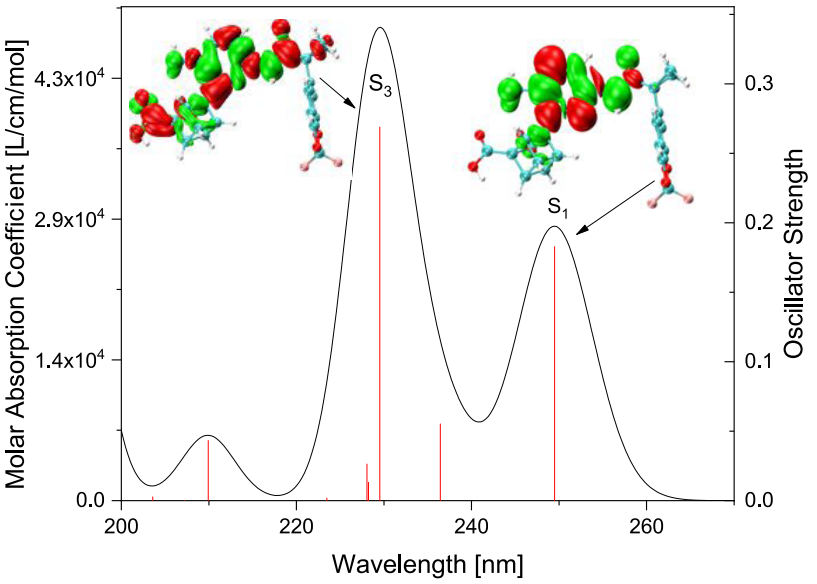

Figure 11. Absorption spectrum of cuba-lumacaftor. The insets are the CDDs, where green and red stand for holes and electrons, respectively, on optical excitation.

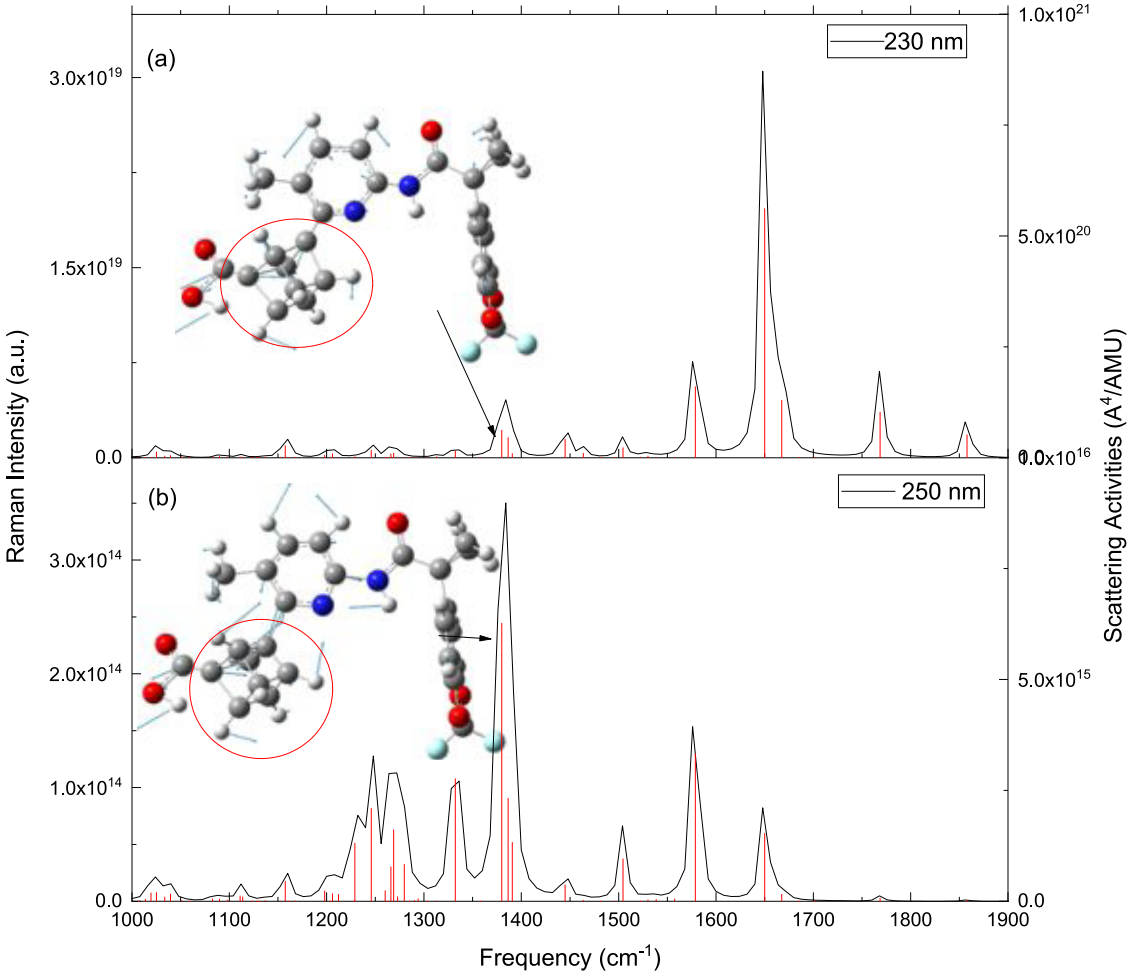

Figure 12. (a, b) Resonance Raman spectra of cuba-lumacaftor in the region from 500 to 2000 cm^{-1}.

enlarged permanent electric dipole moments of cuba-lumacaftor in neutral, acidic, and alkaline environments significantly promote the interaction between cuba-lumacaftor and surrounding polar solvent environments and result in pH-independent high solubility. Raman spectra combined with polarizability demonstrate the vibrational mode information of cuba-lumacaftor. ECD spectra reveal that the chirality of cuba-lumacaftor is much decreased compared to that of lumacaftor.

https://doi.org/10.1021/acsomega.3c07532
ACS Omega 2023, 8, 43332−43340

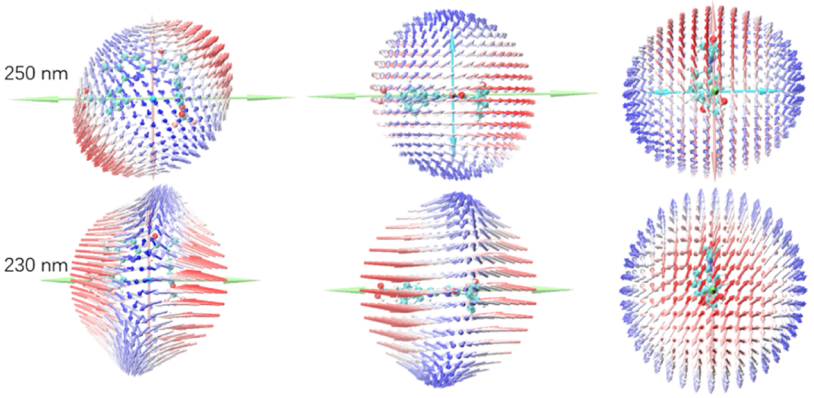

Figure 13. Dynamic polarizability of cuba-lumacaftor excited by 250 and 230 nm in three different orientations.

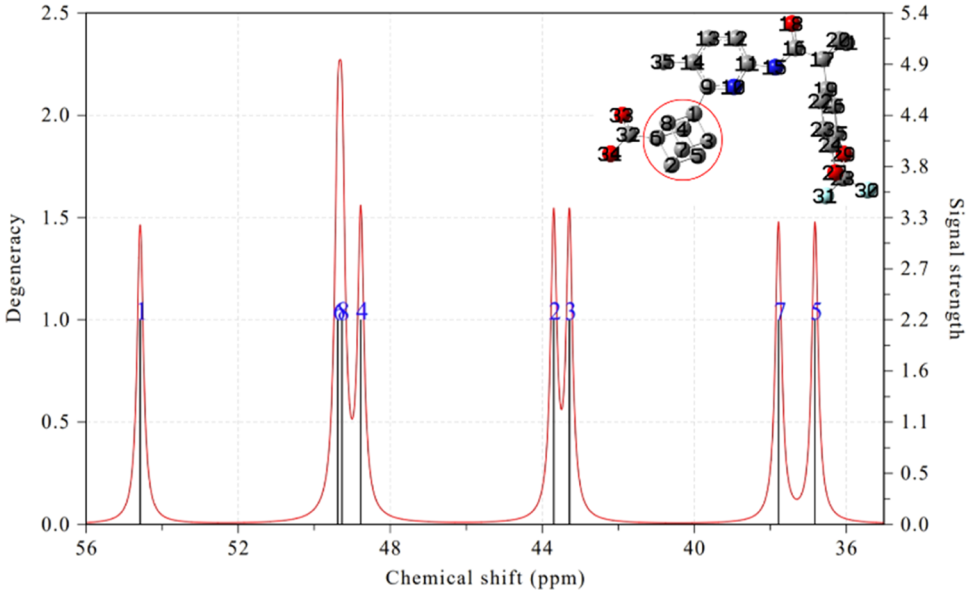

Figure 14. NMR spectra of cuba-lumacaftor about the cubane unit.

AUTHOR INFORMATION

Corresponding Authors

Mengtao Sun − *School of Mathematics and Physics, University of Science and Technology Beijing, Beijing 100083, China;* orcid.org/0000-0002-8153-2679; Email: mengtaosun@ustb.edu.cn

Yongqiang Liang − *Department of Central Sterile Supply, The First Affiliated Hospital of Jinzhou Medical University, Jinzhou, Liaoning 121004, China;* Email: yongqiangliang2023@163.com

Authors

Dongdong Wang − *Department of Radiology, The First Affiliated Hospital of Jinzhou Medical University, Jinzhou, Liaoning 121004, China*

Xiaohong Lyu − *Department of Radiology, The First Affiliated Hospital of Jinzhou Medical University, Jinzhou, Liaoning 121004, China*

Complete contact information is available at: https://pubs.acs.org/10.1021/acsomega.3c07532

Author Contributions

‖D.W. and X.L. contributed equally to this work.

Notes

The authors declare no competing financial interest.

ACKNOWLEDGMENTS

This work was supported by the National Science Foundation of China (11874407, 91436102, and 11374353) and the Fundamental Research Funds for the Central Universities (06500067).

REFERENCES

(1) Deeks, E. D. Lumacaftor/Ivacaftor: A Review in Cystic Fibrosis. *Drugs* **2016**, *76*, 1191−201.

(2) Linsdell, P. Cystic fibrosis transmembrane conductance regulator (CFTR): Making an ion channel out of an active transporter structure. *Channels* **2018**, *12*, 284−290.

(3) Davis, P. B.; Yasothan, U.; Kirkpatrick, P. Ivacaftor. *Nat. Rev. Drug Discovery* **2012**, *11*, 349−350.

(4) Subbaiah, M. A. M.; Meanwell, N. A. Bioisosteres of the Phenyl Ring: Recent Strategic Applications in Lead Optimization and Drug Design. *J. Med. Chem.* **2021**, *64*, 14046−14128.

(5) Wiesenfeldt, M. P.; Rossi-Ashton, J. A.; Perry, I. B.; Diesel, J.; Garry, O. L.; Bartels, F.; Coote, S. C.; Ma, X.; Yeung, C. S.; Bennett, D. J.; MacMillan, D. W. C. General Access to Cubanes as Benzene Bioisosteres. *Nature* **2023**, *618*, 513−518.

(6) Gianatassio, R.; Lopchuk, J. M.; Wang, J.; Pan, C.; Malins, L. R.; Prieto, L.; Brant, T. A.; Collins, M. R.; Gallego, G. M.; Ssch, N. W.; Spangler, J. E.; Zhu, H.; Zhu, J.; Baran, P. S. Strain-release amination. *Science* **2016**, *351*, 241−246.
(7) Zhang, X.; Smith, R. T.; Le, C.; McCarver, S. J.; Shireman, B. T.; Carruthers, N. I.; MacMillan, D. W. C. Copper-mediated synthesis of drug-like bicyclopentanes. *Nature* **2020**, *580*, 220−226.
(8) Eaton, P. E. Cubanes: Starting Materials for the Chemistry of the 1990s and the New Century. *Angew. Chem., Int. Ed.* **1992**, *31*, 1421−1436.
(9) Reekie, T. A.; Williams, C. M.; Rendina, L. M.; Kassiou, M. Cubanes in Medicinal Chemistry. *J. Med. Chem.* **2019**, *62*, 1078−1095.
(10) Lovering, F.; Bikker, J.; Humblet, C. Escape from Flatland: Increasing Saturation as an Approach to Improving Clinical Success. *J. Med. Chem.* **2009**, *52*, 6752−6756.
(11) Biegasiewicz, K. F.; Griffiths, J. R.; Savage, G. P.; Tsanaktsidis, J.; Priefer, R. Cubane: 50 Years Later. *Chem. Rev.* **2015**, *115*, 6719−6745.
(12) Eaton, P. E.; Cole, T. W. Cubane. *J. Am. Chem. Soc.* **1964**, *86*, 3157−3158.
(13) Frisch, M. J.; Trucks, G. W.; Schlegel, H. B.; Scuseria, G. E.; Robb, M. A.; Cheeseman, J. R.; Scalmani, G.; Barone, V.; et al. *Gaussian 16*; Gaussian, Inc.: Wallingford, CT, 2016.
(14) Kohn, W.; Sham, L. J. Self-Consistent Equations Including Exchange and Correlation Effects. *Phys. Rev.* **1965**, *140*, A1133−A1138.
(15) Becke, A. D. Density-functional exchange-energy approximation with correct asymptotic behavior. *Phys. Rev. A* **1988**, *38*, 3098−3100.
(16) Dunning, T. H., Jr Gaussian basis sets for use in correlated molecular calculations. I. The atoms boron through neon and hydrogen. *J. Chem. Phys.* **1989**, *90*, 1007−1023.
(17) Gross, E. K. U.; Kohn, W. Local density-functional theory of frequency-dependent linear response. *Phys. Rev. Lett.* **1985**, *55*, 2850−2852.
(18) Yanai, T.; Tew, D. P.; Handy, N. C. A new hybrid exchange−correlation functional using the Coulomb-attenuating method (CAM-B3LYP). *Chem. Phys. Lett.* **2004**, *393*, 51−57.
(19) Jorge, F. E.; Jorge, S. S.; Suave, R. N. Electronic Circular Dichroism of Chiral Alkenes: B3LYP and CAM-B3LYP Calculations. *Chiarality* **2015**, *27*, 23−31.
(20) Pescitelli, G.; Good, B. T. Computational Practice in the Assignment of Absolute Configurations by TDDFT Calculations of ECD Spectra. *Chirality* **2016**, *28*, 466−474.
(21) Blaser, H. U. Chirality and its implications for the pharmaceutical industry. *Rend. Fis. Accad. Lincei* **2013**, *24*, 213−216.
(22) Brown, C. *Smith Kline Beecham Pharmaceuticals, Welwyn, Hertfordshire, Chirality in Drug Design and Synthesis*; Academic Press: UK, 1990.

https://doi.org/10.1021/acsomega.3c07532
ACS Omega 2023, 8, 43332−43340